Optical Constants of Organic Tholins Produced in a Simulated Titanian Atmosphere: From Soft X-Ray to Microwave Frequencies

B. N. KHARE AND CARL SAGAN

Laboratory for Planetary Studies, Cornell University, Ithaca, New York 14853

E. T. ARAKAWA, F. SUITS, T. A. CALLCOTT, AND M. W. WILLIAMS

Oak Ridge National Laboratory, Oak Ridge, Tennessee 37830

As part of a continuing series of experiments on the production of dark reddish organic solids, called tholins, by irradiation of cosmically abundant reducing gases, the synthesis from a simulated Titanian atmosphere of a tholin with a visible reflection spectrum similar to that of the high altitude aerosols responsible for the albedo and reddish color of Titan has been reported (C. Sagan and B. N. Khare, 1981, *Bull. Amer. Astron. Soc.* **13**, 701; 1982, *Orig. Life.* **12**, 280) and [C. Sagan, B. N. Khare, and J. Lewis, in press. In *Saturn* (M. S. Matthews and T. Gehrels, Eds.), Univ. of Arizona Press, Tucson]. The determination of the real (n) and imaginary (k) parts of the complex refractive index of thin films of such tholin prepared by continuous D.C. discharge through a 0.9 N_2/0.1 CH_4 gas mixture at 0.2 mb are reported. For 250 Å $\leq \lambda \leq$ 1000 μm, n and k have been determined from a combination of transmittance, specular reflectance, interferometric, Brewster angle, and ellipsometric polarization measurements; experimental uncertainties in n are estimated to be ±0.05, and in k ± 30%. Values of n ($\approx$1.65) and k ($\approx$0.004 to 0.08) in the visible range are consistent with deductions made by ground-based and spacecraft observations of Titan. Maximum values of k ($\approx$0.8) are near 1000 Å, and minimum values ($\approx$4 × 10^{-4}) are near 1.5 μm. Many infrared absorption features are present in $k(\lambda)$, including the 4.6-μm nitrile band. © 1984 Academic Press, Inc.

INTRODUCTION

The Voyager 1 discovery (or confirmation) of nine simple organic molecules as minor constituents of the atmosphere of Titan (Hanel *et al.*, 1981; Maguire *et al.*, 1981; Kunde *et al.*, 1981), surmounting an unbroken dark reddish haze layer (Smith *et al.*, 1981), tends to confirm earlier suggestions of an organic aerosol on Titan produced *in situ* from the major atmospheric constituents (Sagan, 1971, 1973, 1974; Khare and Sagan, 1973). In experiments previously reported, we have exposed a simulated Titanian atmosphere [0.09 CH_4/0.91 N_2 at 73 mb] to high-frequency electrical discharge for 4 months and have produced a dark red solid that we propose is similar to the observed Titan aerosol (Sagan and Khare, 1981, 1982; Sagan *et al.*, 1984). Similar

solids, called tholins, are produced by the irradiation of a wide variety of cosmically abundant reducing gases (Sagan and Khare, 1979). The tholin produced at Cornell exhibits a visible spectrum short of the onset at 0.63 μm of the CH_4 Kuiper bands very similar to that observed for the Titan aerosols (Khare *et al.*, 1981; Sagan *et al.*, 1984). Gas chromatography/mass spectrometry of pyrolyzates prepared from this tholin reveals over 75 separate compounds, including many molecules of fundamental biological significance on Earth (Khare *et al.*, 1982, 1983).

A determination of the complex refractive index of various kinds of simulated Titan tholins over as wide a frequency range as possible would permit comparison with refractive index estimates made at visible wavelengths from ground-based and space-

craft photometric and polarimetric observations; would allow calculations on the transmissivity of the Titan atmosphere to sunlight, and therefore on the validity of greenhouse mechanisms to explain the small increment ($\approx 13°C$) of Titan surface temperature over Titan equilibrium temperature; would enable modeling of observed albedo/color variations both in space and in time in the aerosols of Titan; and might be useful for calculations of radiative transfer in the infrared and microwave regimes. Knowledge of the optical properties is also an essential prerequisite for putting on a firmer basis the idea that Titan tholin aerosols are in fact the major chromophore in the atmosphere of Titan.

Reliable determination of the real part, n, and the imaginary part, k, of the complex refractive index of the tholin by measuring the reflectivity of optically thick samples (pressed pellets) and then performing a Kramers–Kronig analysis proved extremely difficult, because the surface of the samples were not truly specular. It became evident that reliable determinations of n and k would require transmission measurements, which in turn would require the preparation of optically thin films of Titan tholin.

Thin films of tholin were generated from a gas mixture of 0.9 N_2 and 0.1 CH_4 by volume at a total pressure of 0.2 mb. This corresponds to a radial distance from the center of Titan of about 2825 km, just at the top of the main cloud deck viewed by Voyagers 1 and 2, and below most of the visible aerosol haze. The solar ultraviolet flux at $\lambda <$ 900 Å, Saturn magnetospheric electrons and protons, solar wind electrons, and cosmic rays are all able to break N_2 chemical bonds and synthesize nitrogenous organics from N_2/CH_4 atmospheres. Saturn magnetospheric particles and interplanetary electrons deposit most of their energy at radial distances between 3200 and 3600 km from the center of Titan (Sagan and Thompson, 1984), a region corresponding to an observed extreme uv opacity in the Titanian

atmosphere (Smith *et al.*, 1982). Cosmic rays and, to a lesser extent, Saturn magnetospheric electrons deposit most of their energy in the Titanian lower atmosphere, at an altitude still inaccessible to observation (Sagan and Thompson, 1984). Thus the tholins produced in the present study are likely to correspond to the reddish aerosol haze in the upper atmosphere of Titan. In the region simulated, at the base of the Titanian thermosphere, the ambient temperatures are $\approx 170°K$. The laboratory experiments were carried out at room temperature, but because the difference in effective temperature between the energy source for molecular dissociation and the ambient temperature is so large, both in the laboratory and on Titan, the choice of laboratory ambient temperatures may not affect the results significantly.

A Technics Hummer V film deposition chamber at Oak Ridge National Laboratory was employed. The experimental setup is shown in Fig. 1, and the details of the electrode and field configurations are given in Fig. 2. The apparatus consists essentially of two horizontal aluminum electrodes of diameter ≈ 7.6 cm, separated by a vertical distance of ≈ 5.7 cm, enclosed coaxially within a vertical glass cylinder of internal diameter ≈ 10 cm. Clean glass or alkali halide substrates for the tholin films were placed in a nearly vertical position on the lower electrode and leaning against the inside wall of the cylindrical glass reaction vessel. The N_2 used was prepared from liquid nitrogen of minimum purity 99.997%, containing <3 ppm H_2O and <5 ppm O_2; the CH_4 was chemically pure (CP) grade, 99% purity. A typical analysis of CP grade methane revealed 0.6% N_2, 0.5% O_2, 0.2% CO and CO_2, and 0.13% C_2H_4 as impurities. Both gases were obtained from Linde Division, Union Carbide Corporation. The gas mixture continuously flowed through the 1-liter chamber at a rate ≈ 0.05 cc/sec. A 15-mA direct current electrical discharge was maintained by a 200-V potential difference between the electrodes. The tholins pre-
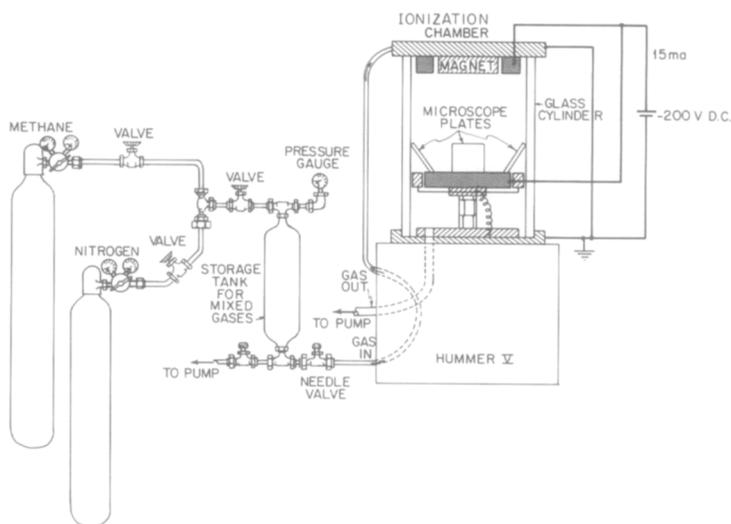
FIG. 1. Experimental apparatus, incorporating Technics "Hummer V" film deposition chamber, used in preparing thin film of Titan tholin on various substrates.

sumably form by quenching and reaction of the ionization and dissociation products in the region of the discharge, and then diffuse outward, where they are deposited on the substrates. Most of the films were formed on glass microscope slides, but some were deposited on disks of CaF_2, LiF, or CsI. Since the substrates were of different sizes, the geometry for film formation varied. The thickness at each point of a given film depends on this geometry, on the deposition time and on the time-variable configuration of the discharge. Thus the thickness varied across each film, and the maximum thickness varied from film to film. A comparatively thick film, with maximum thickness about 20 μm, was deposited in about 3 days of sparking. To obtain the tholin optical constants from the soft X-ray to the microwave region, independent measurements of transmittance, reflectance, interference, and polarization were made, as appropriate.

A general transmission equation for radiation impinging at normal incidence on a thin, absorbing plane-parallel and homogeneous film, separating two nonabsorbing semi-infinite media, one being a substrate

and the other being air or vacuum, is given by Hall and Ferguson (1955). We consider a wavelength region in which a thin homogeneous tholin film characterized by a thickness, t, and a real part, n, of the complex refractive index is transparent, interference fringes are seen, and the normal incidence transmittance T at wavelength λ is

$$T = [1 + 4R_f^2(1 - R_f^2)^{-2} \sin^2 (2\pi nt/\lambda)]^{-1}, \quad (1)$$

where R_f is the reflectance of the tholin film. Maxima in T occur at integer values of $2nt/\lambda$. For wavelength regions in which such a film, deposited on a substrate of thickness t_s, is absorbing, the normal-incidence transmittance is

$$T = (I - R)e^{-\alpha_s t_s}e^{-4\pi kt/\lambda}, \quad (2)$$

where R is the total normal-incidence reflectance from the film–substrate system, α_s is the absorption coefficient (units, cm^{-1}) for the substrate, and k is the imaginary part of the complex refractive index.

The transmittance of substrate alone is

$$T_s = e^{-\alpha_s t_s}(1 - R_0)^2, \quad (3)$$

where R_0 is the normal-incidence reflectance at the substrate–air interface. From
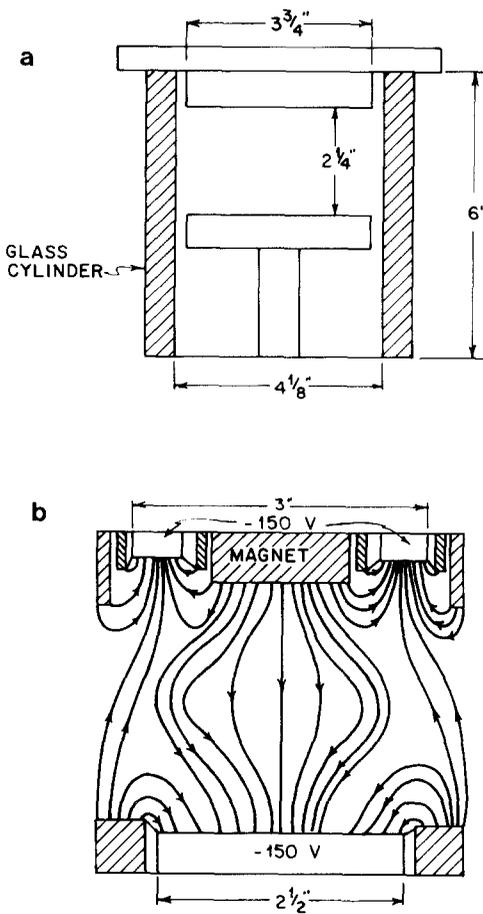
FIG. 2. Ionization chamber. Slides are placed on the bottom electrode and touch the glass walls of the cylinder. (See Fig. 1.) (b) Detail of electrode. Approximate field configuration. All parts are grounded unless otherwise noted.

Eqs. (2) and (3),

$$k = (\lambda/4\pi t) \ln \{[T_s(1 - R)/T]$$
$$[1 - R_0]^{-2}\}, \quad (4)$$

or, if the substrate contributes no extinction,

$$k = (\lambda/4\pi t) \ln [(1 - R)/T]. \quad (5)$$

Values of T_s, R_0, and R can be calculated, as required, from the Fresnel equations and a knowledge of the refractive indices n and n_s of the tholin and the substrate, respectively. Values of n_s for the substrates are known from independent measurements or from the literature (Kaye and Laby, 1966).

In certain wavelength ranges, T_s was measured directly.

Ideally, to obtain k at a given wavelength from a measurement of the transmittance T using Eq. (4) or (5), it is necessary to know t and n independently. In our experiments, for each measurement of T, the thickness t was measured at the same location on the film. In two wavelength ranges, the visible and the far infrared, a direct measurement of n was possible. At other wavelengths an approximate value was first assumed in calculating R. Fortunately, when k is small, an independent measurement of n can be obtained, in which case the values of R_0 and R may significantly affect the calculated value of k. Furthermore, n tends to vary slowly from about 1000 Å to the microwave region. Thus, for wavelengths at which n is not measured directly, a satisfactory estimate can be made for use in the calculation of k.

Over the wavelength range studied, k varies by nearly four orders of magnitude. Thus to obtain optimum sensitivity in measurements of transmittance, we must use films of different thicknesses in different wavelength ranges. The thinnest films employed, which appeared to the naked eye as faint brownish coatings, had central thicknesses of $\simeq 0.6$ μm; the thickest, $\simeq 20$ μm. The film thickness on a given slide tended to increase from the periphery to the center. With all controllable parameters fixed, film thicknesses and geometries still varied from case to case, because of irreproducibilities in the discharge itself. The films, nevertheless, appeared to be homogeneous in color. For each region of the spectrum studied, a large number of samples was prepared and measured, and the results for the complex refractive index presented here are composites of many different observations.

Transmittance measurements were made for 0.15 μm $\leq \lambda \leq 70$ μm and for 100 μm $\leq \lambda \leq 1$ mm. Between 0.15 and 0.5 μm, the transmittances of films with thicknesses from 0.6 to 1 μm deposited on quartz,

CaF_2, or LiF substrates were measured using a Seya-Namioka monochromator. The substrates were small disks about 2.5 cm in diameter. During film deposition, half the substrate was shielded. Transmission measurements were then made through the substrate alone and through the substrate plus tholin. The thickness of the tholin film could be estimated by counting the interference fringes visible using monochromatic light in going from the region of the disk with no film to the region of uniform tholin film thickness. When all measurements of $T_s (\lambda)$ and $T (\lambda)$ had been completed on a given film, the thickness of the film was measured: It was scored at the point where the transmittance was measured, and the film thickness determined at the scratch with a Zeiss light-section microscope, to within ± 0.2 μm, or with a Sloan interferometric microscope, to roughly ± 0.02 μm.

For 0.4 μm $\leq \lambda \leq$ 2.5 μm, tholin samples were deposited on glass microscope slides, placed with one long edge ($\simeq 7.6$ cm) resting on the lower electrode of the reaction vessel. The part of the film deposited along the center of the slide, parallel to the lower electrode, was used for transmittance measurements, each film providing a range of thicknesses along its center line. For each chosen wavelength, T was measured at 6.4-mm intervals using a Cary Model 14PM spectrophotometer, equipped with a movable rack in the sample chamber to accept a microscope slide. Once a sample was inserted, the data taking was fully automated for 19 wavelengths in the 0.4- to 2.5-μm range. Once all the transmission measurements had been recorded, the film was scratched down the middle of the slide, and the thickness along the scratch measured. On a typical film, measured thicknesses ranged from $\simeq 1$ μm at the periphery to $\simeq 20$ μm at the center of the slide.

For 2.5 μm $\leq \lambda \leq$ 40 μm, CaF_2, LiF, and CsI disks were used as substrates. LiF and CaF_2 are opaque beyond 6 and 9 μm, respectively, but CsI transmits well from 2.5 to 50 μm. As with the quartz, CaF_2, and

LiF substrates, half of the CsI substrate was then shielded, so that no film would be deposited on it. Transmittance measurements were obtained using a Perkin–Elmer Model 521 ir spectrometer through CsI alone, and through CsI plus tholin. Transmittance measurements for samples deposited on CsI substrates and on substrates alone were obtained at 2 μm $\leq \lambda \leq$ 70 μm at the NASA Goddard Space Flight Center (GSFC) using a Nicolet Series 8000 Fourier transform ir spectrometer.

Finally, for 100 μm $\leq \lambda \leq$ 1000 μm, pressed pellets were used. Tholin, deposited on the glass wall of the reaction vessel, was scraped off and compacted at 1700 bar into 13-mm-diameter pellets, as described elsewhere (Khare and Sagan, 1979). Three pellets were employed, with thicknesses 0.31, 0.485, and 0.810 mm, as measured using a micrometer caliper. Transmittance was measured at GSFC with the same spectrometer.

Transmittance in the region 70 to 100 μm was interpolated, since at these wavelengths all pellets were too thick and all films were too thin for reliable measurements of transmittance. However, since no spectral feature was found in the reflection study of the pellets in this region, the transmittance interpolation should not introduce serious error.

Ellipsometric polarization measurements (see, e.g., Inagaki, et al., 1976) were performed on thick tholin films in the range 0.4 μm $\leq \lambda \leq$ 2 μm, where k is very small, yielding values varying from $n = 1.7$ at 0.4 μm to 1.6 at 2 μm. Values of n for thin tholin films on substrates of CaF_2, quartz, and glass were also measured directly by the Brewster angle method, as modified by Abeles (1950) for thin, transparent films on substrates. These measurements gave $n \simeq$ 1.63 for 0.4 μm $\leq \lambda \leq$ 0.6 μm. Observations of interference effects in the normal incidence $T (\lambda)$ for thin tholin films on glass yielded $n \simeq 1.7$ between 1.0 and 2.3 μm. The pressed pellets also showed interference patterns in $T (\lambda)$ for 300 μm $\leq \lambda \leq$
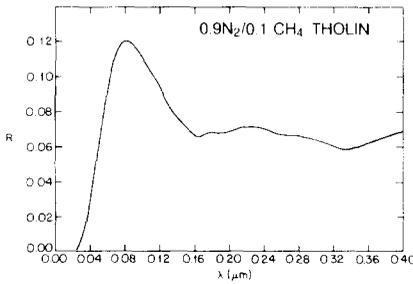
FIG. 3. Normal incidence reflectance of Titan tholin measured as a function of wavelength.

1000 μm, implying $n \approx 2.0$ in this wavelength region.

Reflectance at near-normal incidence, R, was obtained using tholin samples deposited on glass slides. Between 0.025 and 0.13 μm, a McPherson Model 247 grazing incidence monochromator was used, while from 0.13 to 0.4 μm the Seya-Namioka monochromator was employed. The values of R obtained are shown in Fig. 3.

Analysis of the data described in the foregoing paragraphs was performed by means of two separate Kramers–Kronig analyses. For 250 Å $\leq \lambda \leq$ 1500 Å, the absorption in the tholin was too large to obtain k from transmittance measurements; thus, the experimental reflectances, from 0.4 μm (3.1 eV) to 0.025 μm (50 eV), were analyzed to yield tholin n and k values over this wavelength (energy) range by employing the Kramers–Kronig relation between $\theta(E)$, the phase change on reflection at energy E, and the normal incidence reflectance R (see, e.g., Jahoda, 1957):

$$\theta(E) = \frac{E}{\pi} \int_0^\infty \frac{\ln R\,(E')}{(E')^2 - E^2}\, dE'. \quad (6)$$

In addition,

$$\theta(E) = \arctan\left[2k/(1 - n^2 - k^2)\right] \quad (7)$$

and

$$R = [(n - 1)^2 + k^2]/[(n + 1)^2 + k^2]. \quad (8)$$

Thus a determination of $\theta(E)$ from R by means of Eq. (6) allows n and k to be determined from Eqs. (7) and (8); i.e.,

$$n = (1 - R)/(1 + R - 2R^{1/2} \cos \theta)$$

and

$$k = -2R^{1/2} (\sin \theta)/(1 + R - 2R^{1/2} \cos \theta).$$

Since film reflectances were measured only from 3.1 to 50 eV, it was necessary to extrapolate the reflectance to lower and higher energies. From 0 to 3.1 eV, a constant value, equal to the measured value at 3.1 eV, was assumed for R. Because the energies are so low at $E < 3.1$ eV, the values of k for $E > 3.1$ eV, obtained from the Kramers–Kronig analysis, are not very sensitive to this assumption. (Final values of k, derived below, exhibit significant variation with wavelength, and the anticipated infrared spectral features.) Above 50 eV, an exponential extrapolation, $R = R(50)$ $\exp[-0.135\ E]$, was assumed, where $R(50)$ is the measured value at 50 eV, and E is in electron volts. The value of the exponent was equal to the slope on a semi-log plot of the measured near-normal-incidence reflectance, R vs E, above ≈ 25 eV. The integration in Eq. (6) was not carried to infinity. Instead, a high-energy cutoff of 175 eV was chosen to make the calculated k values equal to the experimentally determined k values at the highest energies at which k was measured, i.e., in the region from ≈ 0.2 μm (6.2 eV) to 0.15 μm (8.3 eV). The reflectance data were also analyzed using a power law rather than an exponential extrapolation for $E > 50$ eV. Values of k in the region of high absorption, where k could not be measured directly, were found to be the same with either extrapolation.

The values of k from 0.025 to 0.15 μm, obtained from the Kramers–Kronig analysis of R, were then combined with the experimentally determined k values at longer wavelengths and the interpolated values between 70 and 100 μm. The entire k spectrum is shown in Fig. 4, and tabulated in Table I. The Kramers–Kronig relation between n and k (see, e.g., Inagaki et al., 1977), given by the dispersion relation

TABLE I

REAL (n) AND IMAGINARY ($k \equiv a\ 10^{-b}$) PARTS OF THE COMPLEX REFRACTIVE INDEX OF THOLINS MADE FROM 0.9 N$_2$/0.1 CH$_4$

λ (μm)	k		n	λ (μm)	k		n
	a	b			a	b	
920.0	3.0	3	2.17	2.938	6.0	2	1.59
850.0	1.0	2	2.17	2.818	2.4	2	1.58
774.9	2.9	2	2.16	2.743	1.1	2	1.59
688.8	4.7	2	2.16	2.695	4.1	3	1.60
563.5	7.0	2	2.15	2.422	1.2	3	1.62
387.4	1.0	1	2.12	2.403	8.5	4	1.62
229.6	1.4	1	2.07	2.393	8.0	4	1.62
172.2	1.6	1	2.04	2.214	8.9	4	1.63
140.9	1.6	1	2.03	2.019	7.2	4	1.63
121.5	1.9	1	2.02	1.873	5.2	4	1.63
81.57	2.1	1	1.93	1.823	4.4	4	1.64
56.35	1.9	1	1.86	1.813	4.2	4	1.64
36.46	1.5	1	1.81	1.802	4.0	4	1.64
31.00	1.4	1	1.81	1.381	4.1	4	1.64
22.14	1.8	1	1.80	1.357	4.2	4	1.64
18.23	2.1	1	1.76	1.192	5.2	4	1.65
17.71	2.1	1	1.74	1.148	6.4	4	1.65
14.42	1.7	1	1.67	1.016	1.0	3	1.65
12.91	1.4	1	1.67	0.8731	2.4	3	1.66
11.70	9.7	2	1.64	0.6888	8.8	3	1.68
11.07	7.9	2	1.66	0.5635	2.3	2	1.70
10.51	7.5	2	1.67	0.4428	6.0	2	1.72
8.731	9.2	2	1.71	0.4133	7.6	2	1.69
7.653	1.3	1	1.72	0.3874	9.1	2	1.66
7.044	1.7	1	1.69	0.3542	1.1	1	1.63
6.666	2.2	1	1.69	0.3263	1.3	1	1.64
6.457	2.6	1	1.64	0.2952	1.5	1	1.66
6.326	2.8	1	1.58	0.2638	1.8	1	1.68
5.961	1.5	1	1.43	0.2384	2.1	1	1.68
5.848	7.0	2	1.44	0.1968	2.2	1	1.66
5.740	2.9	2	1.48	0.1631	2.4	1	1.65
5.438	1.1	2	1.55	0.1362	2.7	1	1.70
5.253	8.7	3	1.58	0.1215	3.7	1	1.74
5.166	7.6	3	1.58	0.1181	4.0	1	1.75
4.881	1.0	2	1.61	0.1159	4.3	1	1.75
4.626	2.7	2	1.62	0.1097	5.0	1	1.72
4.592	2.8	2	1.61	0.1016	5.8	1	1.67
4.492	1.4	2	1.61	0.0925	6.7	1	1.58
4.428	1.1	2	1.61	0.0800	7.7	1	1.37
4.217	1.0	2	1.63	0.0785	7.7	1	1.33
3.948	1.3	2	1.64	0.0588	6.2	1	0.963
3.668	2.1	2	1.65	0.0449	3.8	1	0.812
3.463	3.5	2	1.65	0.0415	3.1	1	0.802
3.246	5.6	2	1.65	0.0312	1.4	1	0.850
3.009	7.5	2	1.61	0.0207	4.9	2	0.920

$$n(E) - 1 = \frac{2}{\pi} \int_0^\infty \frac{E'k(E')}{(E')^2 - E^2}\, dE', \quad (9)$$

was then used to obtain n over the entire range from 0.025 to 1000 μm. To perform the integration in Eq. (8), the k (λ) values
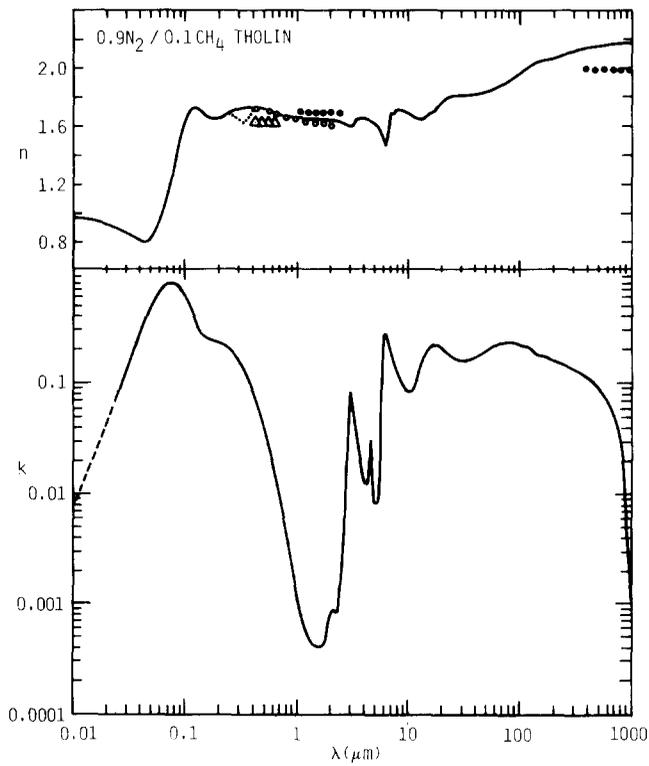
FIG. 4. Real, *n*, and imaginary, *k*, values of the complex refractive index of Titan tholins as a function of wavelength. Determined by Kramers–Kronig analysis (—). Also shown are *n* values obtained independently by ellipsometry (○), from interference patterns in transmission (●), from Brewster angle measurements (△), and from measured *R* and *k* values (···). The dotted curve (···) between 0.2 and 0.4 μm is discussed in the text. The straight dashed line (---) at λ < 0.025 μm is used for the Kramers–Kronig analysis and is also discussed in the text.

were extrapolated at λ < 0.025 μm, as shown by the straight dashed line in Fig. 4. The short wavelength cutoff for this Kramers–Kronig integration was adjusted to make the calculated values of *n* agree with the measured values in the 0.4- to 2.3-μm-wavelength region. The *n* values obtained from the Kramers–Kronig analysis of *k* are exhibited as the solid curve in Fig. 4. However, in the wavelength region from 0.2 to 0.4 μm, the measured reflectance (Fig. 3) shows a structure which was not reproduced by the Kramers–Kronig analyses. This is because the first Kramers–Kronig analysis, performed to obtain *k* values from 0.025 to 0.15 μm, did not reproduce the small values of *k* obtained experimentally from 0.2 to 0.4 μm. In performing the sec-

ond Kramers–Kronig analysis, the measured *k* values from 0.15 to 70 μm and from 100 to 1000 μm, and the interpolated values between 70 and 100 μm were used and the structure present in *R* from 0.2 to 0.4 μm was lost. The values of *n*, calculated using Eq. (7) and the measured values of *R* and *k*, are plotted as the dotted curve in Fig. 4 for 0.2 μm ≤ λ ≤ 0.4 μm. Also shown in Fig. 4 are the independently measured values of *n*. Real parts of refractive indices from the Kramers–Kronig analysis are higher than the measured values in the 300- to 1000-μm-wavelength range, probably because of density differences between the tholin films and pellets.

The normal-incidence Fresnel reflectance, *R*, has been calculated from Eq. (7)

TABLE II

INSTRUMENTS AND TECHNIQUES EMPLOYED IN THE MEASUREMENT OF OPTICAL CONSTANTS OF TITAN THOLINS MADE FROM 0.9 N_2/0.1 CH_4

Wavelength (μm)	Instrument	Measurement		
		Normal reflectance, R, from reflectance	Real part of refractive index, n	Imaginary part of refractive index, k, from transmittance
0.025–9.13	McPherson Model 247 grazing incidence monochromator	X		
0.13–0.15	Seya–Namioka monochromator	X		
0.15–0.4	Seya–Namioka monochromator	X		X
0.4–0.5	Seya–Namioka monochromator		Brewster angle	X
0.5–0.6	Seya–Namioka monochromator		Brewster angle	X
0.4–2.0	Oak Ridge National Laboratory Model HP-E-60/70 ellipsometer		Ellipsometry	
0.4–2.5	Cary Model 14PM spectrometer			X
1.0–2.3	Cary Model 14PM spectrometer		Interferometry	
2.5–40	Perkin–Elmer Model 521 infrared spectrometer			X
2.0–70	Nicolet Series 8000 Fourier transform infrared spectrometer			X
100–300	Nicolet Series 8000 Fourier transform infrared spectrometer			X
300–1000	Nicolet Series 8000 Fourier transform infrared spectrometer		Interferometry	X

for wavelengths above 0.4 μm, and the values plotted in Fig. 5.

To summarize, in the Kramers–Kronig method, n and k can in principle be determined by measuring R over all wavelengths. But it is difficult to make films thick enough to guarantee negligible transmittance at $\lambda > 0.4$ μm, and at $\lambda < 0.025$ μm. Alternatively, k can in principle be measured over all wavelengths by measuring T, and then n extracted by a separate Kramers–Kronig analysis. But, even for our thinnest films, T is too small to measure at $\lambda < 0.15$ μm. Therefore, we have adopted a mixed strategy, the individual measurements for which are summarized in Table II.

FIG. 5. Normal incidence reflectance calculated using the n and k values shown in Fig. 4. The dashed line is due to values of k extrapolated to shorter wavelengths, as shown by the dashed line in Fig. 4. The dotted curve between 0.2 and 0.4 μm is the measured reflectivity plotted in Fig. 3. (See text for details.)

The experimental uncertainties are difficult to evaluate precisely, but are estimated to be ±30% in the measured k values and ±3% in the measured n values. The uncertainty in k arises primarily from sample-to-sample variations. Additional sources of uncertainty in both n and k are small errors in the measurement of reflectance.

So far as we know, values of n and k have never before been obtained over so wide a

wavelength range for any complex organic material. The values of the imaginary part of the refractive index, k, of the tholin vary from almost 1 near 1000 Å to about 3×10^{-4} near 1.5 μm. The slope of k between these two wavelengths—responsible, incidentally, for the red color of the tholin and, presumably, of Titan as well—is due to the superposition of a number of electronic transitions. In the infrared, a number of vibrational transitions are readily identifiable, including C—H near 3 μm and C≡N near 4.6 μm. The infrared spectrum of such tholins are discussed elsewhere (cf. Sagan et al., 1984). From 1000 Å to microwave frequencies, the real part of the refractive index n of the tholin stays approximately constant, wandering sluggishly from ≈ 1.6 to ≈ 2.2, and reflecting in muted fashion the sharper gradients in k, as expected from classical dispersion theory (e.g., Christy, 1972). Shortward of 1000 Å, n falls precipitously to values below 0.8.

Estimates of the real part, n, of the complex refractive index of the Titan aerosol layer, made from ground-based photometric observations (Rages and Pollack, 1980); from Pioneer 11 polarimetric observations (Tomasko and Smith, 1982); and from Voyager photometric observations (Rages and Pollack, 1981, 1983, and private communication), all suggest values for visible wavelengths of 1.65 ± 0.1. In the same wavelength range, our tholins exhibit values $n = 1.65 ± 0.05$, in excellent agreement with ground-based and spacecraft observations. The same Titan observations suggest (see also Rages et al., 1983; Podolak, 1984) values of k in the visible between 0.1 and 0.01, which again corresponds to the values presented here for our CH_4/N_2 tholin. Radiative transfer calculations, to be published separately, reveal a close agreement between the observed spectrum of Titan in the ultraviolet, visible, and near infrared, and the spectrum calculated assuming that the Titan aerosol is composed in significant part of the organic tholin whose complex refractive index is given in Fig. 4.

The experimental program described here may be useful in measuring, with higher accuracy and broader wavelength coverage than has been achieved heretofore, the optical constants of soots and smokes, important for testing the nuclear winter hypothesis (Turco, et al., 1983).

REFERENCES

ABELES, F. (1950). La determination de l'indice et de l'epaisseur des couches minces transparentes. *J. Phys. Radium* **11**, 310–314.

CHRISTY, R. W. (1972). Classical theory of optical dispersion. *Amer. J. Phys.* **40**, 1403–1419.

HALL, J. F., AND W. F. C. FERGUSON (1955). Optical properties of cadmium sulfide and zinc sulfide from 0.6 microns to 14 microns. *J. Opt. Soc. Amer.* **45**, 714–718.

HANEL, R., B. CONRATH, F. M. FLASAR, V. KUNDE, W. MAGUIRE, J. PEARL, J. PIRRAGLIA, R. SAMUELSON, L. HERATH, M. ALLISON, D. CRUIKSHANK, D. GAUTIER, P. GIERASCH, L. HORN, R. KOPPANY, AND C. PONNAMPERUMA (1981). Infrared observations of the Saturnian system from Voyager 1. *Science (Washington, D.C.)* **212**, 192–200.

INAGAKI, T., E. T. ARAKAWA, R. HAMM, AND M. W. WILLIAMS (1977). Optical properties of polystyrene from the near-infrared to the x-ray region and convergence of optical sum rules. *Phys. Rev. B* **15**, 3243–3253.

INAGAKI, T., L. C. EMERSON, E. T. ARAKAWA, AND M. W. WILLIAMS (1976). Optical properties of solid Na and Li between 0.6 and 3.8 eV. *Phys. Rev. B* **13**, 2305–2313.

JAHODA, F. C. (1957). Fundamental absorption of barium oxide from its reflectivity spectrum. *Phys. Rev.* **107**, 1261–1265.

KAYE, G. W. C., AND T. H. LABY (1966). *Tables of Physical and Chemical Constants*, pp. 83–86. Wiley, New York.

KHARE, B. N., AND C. SAGAN (1973). Red clouds in reducing atmospheres. *Icarus* **20**, 311–321.

KHARE, B. N., AND C. SAGAN (1975). Cyclic octatomic sulfur: A possible infrared and visible chromophore in the clouds of Jupiter. *Science (Washington, D.C.)* **189**, 722–723.

KHARE, B. N., C. SAGAN, S. SHRADER, AND E. T. ARAKAWA (1982). Molecular analysis of tholins produced under simulated Titan conditions. *Bull. Amer. Astron. Soc.* **14**, 714.

KHARE, B.N., C. SAGAN, E. T. ARAKAWA, H. OGINO, T. O. WILLINGHAM, AND B. NAGY (1983). Amino acid analysis of Titan tholins. *Bull. Amer. Astron. Soc.* **15**, 843.

KHARE, B. N., C. SAGAN, AND J. GRADIE (1981). Reflection spectra of simulated Titan organic clouds. *Bull. Amer. Astron. Soc.* **13**, 701.

KUNDE, V. G., A. C. AIKEN, R. A. HANEL, D. E. JENNINGS, W. C. MAGUIRE, AND R. E. SAMUELSON (1981). C_4H_2, HC_3N and C_2N_2 in Titan's atmosphere. *Nature (London)* **292**, 686–688.

MAGUIRE, W. C., R. A. HANEL, D. E. JENNINGS, V. G. KUNDE, AND R. E. SAMUELSON (1981). C_3H_8 and C_3H_4 in Titan's atmosphere. *Nature (London)* **292**, 683–686.

PODOLAK, M. (1984). Are the polarization data consistent with constant flux models of Titan's atmosphere? *Icarus* **58**, 325–329.

RAGES, K., AND J. B. POLLACK (1980). Titan aerosols: Optical properties and vertical distribution. *Icarus* **41**, 119–130.

RAGES, K., AND J. B. POLLACK (1981). High phase angle Voyager images of Titan's main aerosol layer. *Bull. Amer. Astron. Soc.* **13**, 703.

RAGES, K., AND J. B. POLLACK (1982). Aerosol extinction profiles in Titan's atmosphere. *Bull. Amer. Astron. Soc.* **14**, 714.

RAGES, K., AND J. B. POLLACK (1983). Vertical distribution of scattering hazes in Titan's upper atmosphere. *Icarus* **55**, 50–62.

RAGES, K., J. B. POLLACK, AND O. B. TOON (1983). Radiative-convective equilibrium temperature profiles in Titan's atmosphere. *Bull. Amer. Astron. Soc.* **15**, 841.

SAGAN, C. (1971). The solar system beyond Mars: An exobiological survey. *Space Sci. Rev.* **11**, 73–112.

SAGAN, C. (1973). The greenhouse of Titan. *Icarus* **18**, 649–656.

SAGAN, C. (1974). Organic Chemistry in the Atmosphere: *The Atmosphere of Titan* (D. M. Hunten, Ed.), NASA Special Publication SP-340, pp. 134–142. U.S. Govt. Printing Office, Washington, D.C.

SAGAN, C., AND B. N. KHARE (1979). Tholins: Organic chemistry of interstellar grains and gas. *Nature (London)* **277**, 102–107.

SAGAN, C., AND B. N. KHARE (1981). The organic clouds of Titan. *Bull. Amer. Astron. Soc.* **13**, 701.

SAGAN, C., AND B. N. KHARE (1982). The organic clouds of Titan. *Orig. Life* **12**, 280.

SAGAN, C., AND W. R. THOMPSON (1984). Production and condensation of organic gases in the atmosphere of Titan. *Icarus* **59**, 133–161.

SAGAN, C., B. N. KHARE, AND J. LEWIS (1984). Organic matter in the Saturn system. In *Saturn* (M. S. Matthews and T. Gehrels, Eds.). Univ. of Arizona Press, Tucson, in press.

SMITH, B., L. SODERBLOM, R. BEEBE, J. BOYCE, G. BRIGGS, A. BUNKER, S. A. COLLINS, C. J. HANSEN, T. V. JOHNSON, J. L. MITCHELL, R. J. TERRILE, M. CARR, A. F. COOK II, J. CUZZI, J. B. POLLACK, G. E. DANIELSON, A. INGERSOLL, M. E. DAVIES, G. E. HUNT, H. MASURSKY, E. SHOEMAKER, D. MORRISON, T. OWEN, C. SAGAN, J. VEVERKA, R. STROM, AND V. E. SUOMI (1981). Encounter with Saturn: Voyager 1 imaging science results. *Science (Washington, D.C.)* **212**, 163–190.

SMITH, G. R., D. F. STROBEL, A. L. BROADFOOT, B. R. SANDEL, D. E. SHEMANSKY, AND J. B. HOLBERG (1982). Titan's upper atmosphere: composition and temperature from the EUV solar occultation results. *J. Geophys. Res.* **87**, 1351–1360.

TOMASKO, M. G., AND P. H. SMITH (1982). Photometry and polarimetry of Titan: Pioneer 11 observations and their implications for aerosol properties. *Icarus* **51**, 65–95.

TURCO, R. P., O. B. TOON, T. P. ACKERMAN, J. B. POLLACK, AND C. SAGAN (1983). Nuclear Winter: Global consequences of multiple nuclear explosions. *Science (Washington, D.C.)* **222**, 1283–1292.